ELSEVIER

Inorganica Chimica Acta 280 (1998) 243–248

Inorganica Chimica Acta

Binuclear and tetranuclear complexes prepared by reactions of dodecacarbonyltriruthenium with the N-substituted cinnamic acid amides. Crystal and molecular structures of $[Ru_2(\mu\text{-}H)(\mu\text{-}\eta^3\text{-}PhC{=}CHC(O)N(CH_2)_4)(CO)_6]$ and $[Ru_4(\mu_3\text{-}H)_2(\mu\text{-}\eta^3\text{-}PhC{=}CHC(O)N(CH_2)_4)_2(CO)_{10}]$

M.I. Rybinskaya *, N.A. Stelzer, L.V. Rybin, F.M. Dolgushin, A.I. Yanovsky, Yu.T. Struchkov [1], P.V. Petrovskii

A.N. Nesmeyanov Institute of Organoelement Compounds, 28 Vavilov Street, 117813 Moscow, Russia

Received 7 October 1997; received in revised form 27 December 1997; accepted 19 February 1998

Dedicated to the memory of Professor M.E. Vol'pin

Abstract

The thermal reactions of $Ru_3(CO)_{12}$ with the N-substituted cinnamic acid amides PhCH=CHCONRR′ (**1**) in hydrocarbons yield the binuclear and tetranuclear complexes, $[Ru_2(\mu\text{-}H)(\mu\text{-}\eta^3\text{-}PhC{=}CHC(O)NRR')(CO)_6]$ (**2**) and $[Ru_4(\mu_3\text{-}H)_2(\mu\text{-}\eta^3\text{-}PhC{=}CHC(O)\text{-}NRR')(CO)_{10}]$ (**3**), involving five-membered oxaruthenacycles η^3 coordinated by the second ruthenium atom. The structures of the complexes were determined by single crystal X-ray diffraction studies. On heating in hydrocarbons, complexes **2** are converted into clusters **3**. The reverse transformation occurs on treatment of complexes **3** by methylene chloride.

Keywords: Crystal structures; Ruthenium complexes; Carbonyl complexes; Cinnamic acid amide complexes

1. Introduction

The present work is the continuation of our studies of reactions between metal carbonyls of the iron subgroup and functionally substituted olefins. Previously we have shown that the presence of substituents at the olefinic carbon atoms changes the course of the reactions and the structures of the products [1]. Thus, rather interesting results were obtained in the studies of reactions of $Ru_3(CO)_{12}$ with unsaturated ketones [2–4]. These reactions yield bi- and polynuclear complexes involving five-membered oxaruthenacycles, η^3 coordinated by the second metal atom and/or η^3 coordinated dihydropyrane ligands formed as a result of the coupling of two starting enone molecules. It seemed especially interesting to study the reactions of $Ru_3(CO)_{12}$ with unsaturated amides which contain the oxadiene system C=C–C=O along with the amino group possessing the lone electron pair and thus having one more potential site of coordination for the metal atom.

In this paper we report the results of our studies of the thermal reactions between $Ru_3(CO)_{12}$ and cinnamic acid amides PhCH=CHC(NRR′)=O (**1a–d**; **a**: R+R′=$(CH_2)_4$; **b**: R=R′=Me; **c**: R=R′=Et; **d**: R=Me, R′=H) in hydrocarbon media.

2. Experimental

All reactions were carried out in an argon atmosphere. The solvents were purified using the standard procedures. The ^1H NMR spectra were recorded with the Bruker WP200SY, IR spectra were registered with a Specord IR-75 spectrometer (Table 1). Elemental analyses were performed at the Institute of Organoelement Compounds (Russia).

*2.1. Reaction of $Ru_3(CO)_{12}$ with **1a***

160 mg (0.25 mmol) of $Ru_3(CO)_{12}$ [5] and 151 mg (0.75 mmol) of **1a** in 80 ml of hexane were refluxed for 6 h.

---

* Corresponding author. Fax: +7-095-135 5085.

[1] Deceased on August 16, 1995.

0020-1693/98/$ - see front matter © 1998 Elsevier Science S.A. All rights reserved.
PII S0020-1693(98)00173-X

Table 1
IR and NMR spectra for complexes **1**, **2** and **3**

Compound	Carbonyl bands [a] (cm^{-1})	^1H NMR [b]
1a		7.62 (d, *J* 15.6, 1H, CH), 7.55–7.25 (m, 5H, Ph), 6.88 (d, *J* 15.6, 1H, CH), 3.71–3.44 (m, 4H, CH_2), 1.71–1.47 (m, 4H, CH_2)
1b		7.66 (d, *J* 15.4, 1H, CH), 7.50–7.30 (m, 5H, Ph), 6.87 (d, *J* 15.4, CH), 3.10 (s, 6H, Me)
1c		7.69 (d, *J* 15.4, 1H, CH), 7.60–7.20 (m, 5H, Ph), 6.81 (d, *J* 15.4, 1H, CH), 3.45 (q, *J* 5.6, 4H, CH_2), 1.19 (t, *J* 5.6, 6H, Me)
1d		7.61 (d, *J* 15.7, 1H, CH), 7.50–7.20 (m, 5H, Ph), 6.76 (s, broad, 1H, NH), 6.53 (d, *J* 15.7, 1H, CH), 2.92 (d, *J* 4.1, 3H, Me)
2a	2098m, 2052vs, 2036m, 2010vs, 1990s, 1974m	7.52–7.10 (m, 5H, Ph), 3.44–3.13 (m, 4H, CH_2), 2.91 (d, *J* 1.3, 1H, CH), 2.00–1.80 (m, 4H, CH_2), −12.58 (d, *J* 1.3, 1H, RuH)
2b	2094m, 2050vs, 2030m, 2010vs, 1990s, 1972m	7.60–7.10 (m, 5H, Ph), 3.04 (s, 3H, Me), 3.00 (d, *J* 1.4, 1H, CH), 2.75 (s, 3H, Me), −12.57 (d, *J* 1.4, 1H, RuH)
2c	2094m, 2050vs, 2032m, 2008vs, 1986s, 1970m	7.60–7.00 (m, 5H, Ph), 3.01 (d, *J* 1.2, 1H, CH), 3.38 (dq, *J* 15.2, 7.6, 2H, 2CH*H*), 3.26 (dq, *J* 15.2, 7.6, 1H, C*H*H), 2.90 (dq, *J* 15.2, 7.6, 1H, C*H*H), 1.27 (t, *J* 7.6, 3H, Me), 1.00 (t, *J* 7.6, 3H, Me), −12.56 (d, *J* 1.2, 1H, RuH)
2d [c]	2094m, 2050vs, 2030m, 2010vs, 1990s, 1970m	7.50–7.10 (m, 5H, Ph), 5.61 (q, *J* 5.0, 1H, NH), 2.95 (d, *J* 1.0, 1H, CH), 2.94 (d, *J* 5.0, 3H, Me), −12.52 (d, *J* 1.0, 1H, RuH)
		7.50–7.10 (m, 5H, Ph), 5.77 (q, *J* 5.0, 1H, NH), 2.94 (d, *J* 1.0, CH), 2.65 (d, *J* 5.0, 3H, Me), −12.38 (d, *J* 1.0, 1H, RuH)
3a [d]	2055, 2025, 1990, 1970, 1955	
3b	2053, 2022, 1991, 1975, 1955	
3c	2053, 2025, 1990, 1975, 1955	
3d	2050, 2024, 1988, 1979, 1964	

[a] In hexane.
[b] In $CDCl_3$.
[c] Two isomers in the approximate ratio 1:5.
[d] Complexes **3a–d** are unstable in solutions, so their IR spectra were measured in Nujol; NMR data are not available.

The reaction mixture was then cooled and filtered. The precipitate was washed with methanol; 14 mg of dark red crystals of **3a** were obtained (yield 7%), its IR spectrum is given in Table 1. The hexane filtrate was chromatographed on the silica gel column with the 3:1 petroleum ether–CH_2Cl_2 mixture as the eluent. 84 mg (40%) of yellow crystals of **2a** were thus obtained. *Anal.* Calc. for $C_{19}H_{15}NO_7Ru_2$: C, 39.93; H, 2.63; N, 2.45. Found: C, 40.12; H, 2.79; N, 2.40%.

2.2. Reaction of $Ru_3(CO)_{12}$ with 1b

160 mg (0.25 mmol) of $Ru_3(CO)_{12}$ and 130 mg (0.75 mmol) of **1b** in 80 ml of hexane were refluxed for 6 h. The reaction mixture was then cooled and filtered. The precipitate was washed with methanol; 45 mg (23%) of complex **3b**, which was identified on the basis of its IR spectrum (Table 1), were obtained. The hexane filtrate was chromatographed on the silica gel column with the 3:1 petroleum ether–CH_2Cl_2 mixture as the eluent. 104 mg (50%) of yellow crystals of **2b** were thus obtained. *Anal.* Calc. for $C_{17}H_{13}NO_7Ru_2$: C, 37.43; H, 2.39; N, 2.57. Found: C, 37.56; H, 2.51; N, 2.70%.

2.3. Reaction of $Ru_3(CO)_{12}$ with 1c

The reaction was carried out in the same way as that with **1a**. 201 mg (47%) of yellow product **2c** were obtained from 320 mg (0.5 mmol) of $Ru_3(CO)_{12}$ and 304 mg (1.5 mmol) of **1c** in 120 ml of hexane. *Anal.* Calc. for $C_{19}H_{17}NO_7Ru_2$: C, 39.79; H, 2.97; N, 2.44. Found: C, 40.03; H, 3.24; N, 2.40%. Dark red crystals of **3c** in trace amounts were located on the walls of the flask; their identification was based on the IR spectrum (Table 1).

2.4. Reaction of $Ru_3(CO)_{12}$ with 1d

320 mg (0.5 mmol) of $Ru_3(CO)_{12}$ and 242 mg (1.5 mmol) of **1d** were refluxed in 120 ml of hexane and then worked up as described for **1a**. 138 mg (30%) of **2d**, isolated in the form of yellow oil and identified on the basis of its IR spectrum, were obtained. The trace amounts of dark red crystals of **3d** (also identified by its IR spectrum, see Table 1) precipitated on the walls of the flask.

2.5. The 2a → 3a transformation

35 mg (0.06 mmol) of **2a** dissolved in 50 ml of hexane were refluxed for 8 h. The colour of the solution changed from yellow to red. After cooling, the reaction mixture was filtered off and the precipitate was washed with methanol. 22 mg (67%) of complex **3a** were obtained; the identification of the complex was carried out on the basis of its IR spectrum.

2.6. The 3a → 2a transformation

22 mg (0.02 mmol) of **3a** were dissolved in 30 ml of CH_2Cl_2 and stirred for 2 h at room temperature. The colour

of the solution changed from red to yellow. The solvent was removed in vacuo. 11 mg (0.02 mmol) of complex **2a**, identified on the basis of its IR spectrum, were isolated.

2.7. X-ray structural studies of 2a and 3a

Details of crystal parameters, data collection and structure refinement for complexes **2a** and **3a** are given in Table 2. Both structures were solved by direct methods and refined by the full-matrix least-squares technique. The hydride atom and the H atom bonded to the C atom involved in the oxaruthenacycle in **2a** were located in the difference Fourier synthesis and refined isotropically; all other H atoms in **2a** were included into least-squares refinement in the riding model approximation. The Flack parameter [6] for **2a** refined to 0.45(11), which does not allow one to assign the absolute structure. All H atoms in **3a** were located in the difference Fourier syntheses and refined isotropically. The calculations were performed with the SHELXTL PLUS 5 programs [7] on an IBM PC computer.

3. Results and discussion

It is known that interactions of $Ru_3(CO)_{12}$ with oxadienes C=C–C=O produce complexes of various nuclearity with the five-membered oxaruthenacycles η^3 coordinated by the second ruthenium atoms as the main structural motif [2,3]. The cinnamic acid amides PhCH=CHC(NRR′)=O (**1a–d**) also contain the oxadiene bond system, but, in contrast to unsaturated ketones studied earlier [2–4], this oxadiene system has a donor amino group attached to the carbonyl function.

Reactions of $Ru_3(CO)_{12}$ with **1a–d** were carried out by heating of the reagents in refluxing hexane. The heating was stopped as soon as $Ru_3(CO)_{12}$ was completely consumed (IR monitoring). The reactions result in the formation of bi- (**2**) and tetranuclear (**3**) complexes containing oxaruthenacycles.

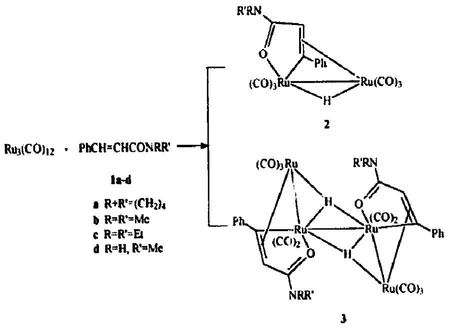

The structures of complexes **2** and **3** became known from the X-ray diffraction studies of **2a** and **3a**. Selected bond lengths and angles in **2a** (Fig. 1) are listed in Table 3. The structure of this complex is similar to that observed earlier for the product of reaction of $Ru_3(CO)_{12}$ with benzylideneacetone [8]. Two ruthenium atoms in **2a** are linked via direct Ru–Ru bond, μ-hydride bridging H atom and former oxadiene ligand which has lost one of its hydrogen atoms. The latter forms the Ru(2)–C(9) covalent and the Ru(2)–O(7) coordination bonds, thus yielding the five-membered chelate oxaruthenacycle; the Ru(1) atom is η^2 coordinated by the olefinic C(8)=C(9) bond.

As pointed out earlier [8], an appreciable electron density delocalization occurs in the C=C–C=O chain of the oxaruthenacycle. Therefore, it seemed worthwhile to trace those changes in the geometry of the ligand which may be attributed to the influence of the amino substituent. Thus, the structural data obtained indicate the presence of conjugation between the lone electron pair of the nitrogen atom and the C=O double bond, which is reflected in the C(7)–N(1) bond length (1.341(12) Å) considerably shortened in comparison with the standard value for C_{sp^2}–N_{sp^3} bond (1.416 Å as quoted in [9]). The amino–carbonyl conjugation is also manifested in the almost coplanar arrangement of the N(1) atom and the carbonyl group environments, the O(7)C(7)N(1)C(10) and O(7)C(7)N(1)C(13) torsion angles being equal to 175.9 and 5.1°, respectively. The influence of the amino nitrogen atom also obviously causes some decrease in the degree of conjugation between the C(7)=O(7) and the C(8)=C(9) double bonds which results in the noticeable elongation of the C(7)–C(8) bond (up to 1.455(13) Å) in comparison with the corresponding bond in the analogous complex, $[Ru_2(\mu\text{-}H)(\mu\text{-}\eta^3\text{-}PhC{=}CHC(O)Me)(CO)_6]$ (**4**), derived from benzylideneacetone (1.411 Å [8]).

One may also conclude that somewhat decreased delocalization in the enone system with the nitrogen-containing sub-

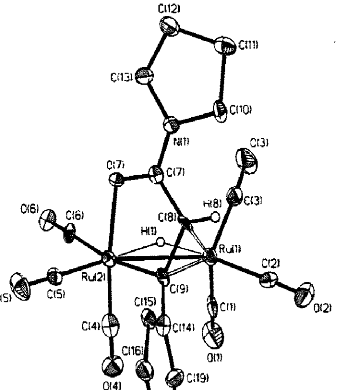

Fig. 1. Molecular structure of complex **2a**. Thermal ellipsoids are drawn at 50% probability level.

Table 2
Details of crystal parameters, data collection and structure refinements for complexes **2a** and **3a**

Compound	**2a**	**3a**
Formula	$C_{19}H_{15}NO_7Ru_2$	$C_{36}H_{30}N_2O_{12}Ru_4$
Molecular weight	571.46	1086.90
Crystal system	orthorhombic	triclinic
Space group	$P2_12_12_1$	P-1
Cell constants		
a (Å)	8.749(7)	9.844(3)
b (Å)	9.517(7)	10.064(3)
c (Å)	24.49(2)	11.233(2)
α (°)	–	91.17(2)
β (°)	–	113.14(2)
γ (°)	–	106.18(2)
V (Å^3)	2039	972.1
Z	4	1
D_{calc} (g cm^{-3})	1.862	1.857
Diffractometer	Siemens P3/PC	Siemens P3/PC
No. reflections for cell determination	24	24
2θ Range (°)	$22 < 2\theta < 23$	$23 < 2\theta < 24$
Temperature (K)	146	153
Radiation	Mo Kα ($\lambda = 0.71073$)	Mo Kα ($\lambda = 0.71073$)
Scan mode	θ–2θ	θ–2θ
$2\theta_{max}$ (°)	62	60
Absorption coefficient μ(Mo Kα) (cm^{-1})	15.21	15.86
Total no. reflections	3678	6008
No. unique reflections	3678	5701
No. reflections used in refinement	3628	5642
No. observed reflections ($I > 2\sigma(I)$)	2283	4469
No. parameters	271	304
R_1 (on F for observed reflections) [a]	0.0663	0.0439
wR_2 (on F^2 for all reflections) [b]	0.1312	0.1221
Goodness of fit	1.096	1.047

[a] $R_1 = \Sigma |F_o - |F_c|| / \Sigma(F_o)$ for observed reflections.

[b] $wR_2 = \{\Sigma[w(F_o^2 - F_c^2)^2] / \Sigma(F_o^2)^2]\}^{1/2}$ for all reflections.

stituent results in the more symmetrical π coordination of the C(8)=C(9) bond by the Ru(1) atom (the difference between the Ru(1)–C(8) and Ru(1)–C(9) bond lengths in **2a** is about 0.08 Å whereas the corresponding difference in **4** is as large as 0.13 Å). At the same time the η^2-coordinated olefinic bond itself (C(8)=C(9)) is not affected by the presence of the amino group, the corresponding bond lengths being almost identical in **2a** and **4** (1.473(12) and 1.468(5) Å, respectively).

The five-membered oxaruthenacycle in **2a** has an envelope conformation similar to that observed in **4** [8]: the displacement of the Ru(2) atom from the mean plane of the remaining four atoms of the cycle in **2a** is equal to 0.495 Å (0.45 Å in **4**). Nevertheless, the O(7)C(7)C(8)C(9) sequence shows much more significant deviation from planarity in **2a** than in **4**, which is reflected in different O(7)C(7)C(8)C(9) torsion angles (7.2 and 2.8°, respectively). The phenyl plane C(14)–C(19) in **2a** is nearly normal to the O(7)C(7)C(8)C(9) plane (76.6°); the corresponding dihedral angle in **4** is equal to 68.4°.

The non-equivalence of the ruthenium–carbonyl bonds in **2a**, which is obviously due to the different *trans* effects of the C, H, and O atoms, is noteworthy. It is manifested in considerable scatter of the Ru–C(CO) bond lengths which span the range from 1.881 to 1.986 Å.

The structure of **3a** was also determined in the X-ray diffraction study (Fig. 2, Table 4). Its molecule involves a planar metal chain made up of four ruthenium atoms, two oxadiene and two hydride ligands as well as ten terminal carbonyl groups. The electron count technique yields 64 valence electrons for **3a** rather than 66e which should have been expected for such a cluster according to the EAN rule. Therefore, complex **3a** represents a rare example of an electron-deficient polynuclear ruthenium complex.

Complex **3a** occupies a special position in the inversion centre which coincides with the mid-point of the Ru(2)–Ru(2A) bond. Each of the symmetry-related halves of the molecule closely resembles binuclear complex **2a** lacking one carbonyl group. These binuclear fragments are linked via an Ru–Ru bond and two μ_3-hydride ligands, some elongation of the Ru(2)–Ru(2A) bond (up to 3.0109(8) Å) being obviously associated with the presence of hydride bridges, which are known to cause an increase in the corresponding metal–metal bond lengths. The Ru(1)–Ru(2) bond is considerably shorter (2.9256(9) Å), which may be attributed to the influence of oxadiene groups simultaneously chelating

Table 3
Selected bond lengths (Å) and angles (°) for **2a**

Ru(1)–C(2)	1.895(9)	Ru(2)–C(9)	2.102(10)
Ru(1)–C(1)	1.904(11)	Ru(2)–O(7)	2.122(6)
Ru(1)–C(3)	1.970(11)	Ru(2)–H(1)	1.87(9)
Ru(1)–C(9)	2.123(8)	N(1)–C(7)	1.341(12)
Ru(1)–C(8)	2.201(10)	N(1)–C(10)	1.459(12)
Ru(1)–Ru(2)	2.871(2)	N(1)–C(13)	1.470(12)
Ru(1)–H(1)	1.72(9)	O(7)–C(7)	1.275(11)
Ru(2)–C(4)	1.881(12)	C(7)–C(8)	1.455(13)
Ru(2)–C(5)	1.915(10)	C(8)–C(9)	1.473(12)
Ru(2)–C(6)	1.986(10)	C(9)–C(14)	1.480(13)
C(2)–Ru(1)–C(1)	92.8(5)	C(4)–Ru(2)–O(7)	172.9(4)
C(2)–Ru(1)–C(3)	98.3(4)	C(5)–Ru(2)–O(7)	93.1(4)
C(1)–Ru(1)–C(3)	102.0(5)	C(6)–Ru(2)–O(7)	90.8(3)
C(2)–Ru(1)–C(9)	96.9(4)	C(9)–Ru(2)–O(7)	82.8(3)
C(1)–Ru(1)–C(9)	113.3(4)	C(4)–Ru(2)–Ru(1)	89.0(3)
C(3)–Ru(1)–C(9)	140.6(5)	C(5)–Ru(2)–Ru(1)	141.3(3)
C(2)–Ru(1)–C(8)	90.2(4)	C(6)–Ru(2)–Ru(1)	123.7(3)
C(1)–Ru(1)–C(8)	153.0(4)	C(9)–Ru(2)–Ru(1)	47.5(2)
C(3)–Ru(1)–C(8)	104.0(5)	O(7)–Ru(2)–Ru(1)	84.0(2)
C(9)–Ru(1)–C(8)	39.8(3)	C(7)–N(1)–C(10)	124.4(8)
C(2)–Ru(1)–Ru(2)	142.9(3)	C(7)–N(1)–C(13)	121.4(8)
C(1)–Ru(1)–Ru(2)	95.5(3)	C(10)–N(1)–C(13)	113.7(8)
C(3)–Ru(1)–Ru(2)	115.0(3)	C(7)–O(7)–Ru(2)	110.2(6)
C(9)–Ru(1)–Ru(2)	46.9(3)	O(7)–C(7)–N(1)	118.8(8)
C(8)–Ru(1)–Ru(2)	67.1(3)	O(7)–C(7)–C(8)	120.7(8)
C(4)–Ru(2)–C(5)	91.7(4)	N(1)–C(7)–C(8)	120.6(8)
C(4)–Ru(2)–C(6)	93.9(4)	C(7)–C(8)–C(9)	117.3(9)
C(5)–Ru(2)–C(6)	94.9(4)	C(8)–C(9)–C(14)	.22.9(8)
C(4)–Ru(2)–C(9)	91.7(4)	C(8)–C(9)–Ru(2)	104.8(7)
C(5)–Ru(2)–C(9)	93.8(4)	C(14)–C(9)–Ru(2)	125.7(6)
C(6)–Ru(2)–C(9)	169.6(4)	Ru(1)–H(1)–Ru(2)	106(4)

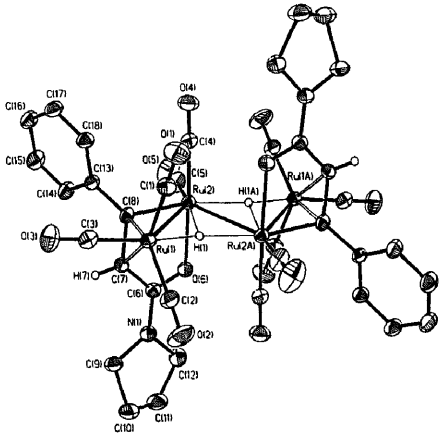

Fig. 2. Molecular structure of complex **3a**. Thermal ellipsoids are drawn at 50% probability level.

the Ru(2) and π coordinating the Ru(1) atom. The long Ru(1)···Ru(2A) distance 3.556(1) Å excludes the possibility of direct bonding between these metal atoms.

Table 4
Selected bond lengths (Å) and angles (°) for **3a**

Ru(1)–C(3)	1.892(4)	Ru(2)–Ru(2A)	3.0109(8)
Ru(1)–C(1)	1.926(4)	Ru(2)–H(1)	1.96(7)
Ru(1)–C(2)	1.974(4)	Ru(1)···Ru(2A)	3.556(1)
Ru(1)–C(8)	2.121(4)	Ru(2A)–H(1)	1.93(7)
Ru(1)–C(7)	2.223(4)	O(6)–C(6)	1.284(5)
Ru(1)–Ru(2)	2.9256(9)	N(1)–C(6)	1.330(5)
Ru(1)–H(1)	1.73(7)	N(1)–C(12)	1.473(5)
Ru(2)–C(5)	1.871(4)	N(1)–C(9)	1.473(6)
Ru(2)–C(4)	1.875(4)	C(6)–C(7)	1.458(5)
Ru(2)–C(8)	2.059(4)	C(7)–C(8)	1.452(5)
Ru(2)–O(6)	2.115(3)	C(8)–C(13)	1.486(5)
C(3)–Ru(1)–C(1)	91.2(2)	C(4)–Ru(2)–Ru(1)	94.05(12)
C(3)–Ru(1)–C(2)	97.3(2)	C(8)–Ru(2)–Ru(1)	46.47(10)
C(1)–Ru(1)–C(2)	101.7(2)	O(6)–Ru(2)–Ru(1)	84.48(8)
C(3)–Ru(1)–C(8)	91.7(2)	C(5)–Ru(2)–Ru(2A)	143.00(14)
C(1)–Ru(1)–C(8)	112.3(2)	C(4)–Ru(2)–Ru(2A)	95.35(12)
C(2)–Ru(1)–C(8)	144.6(2)	C(8)–Ru(2)–Ru(2A)	119.64(10)
C(3)–Ru(1)–C(7)	88.6(2)	O(6)–Ru(2)–Ru(2A)	85.95(8)
C(1)–Ru(1)–C(7)	151.2(2)	Ru(1)–Ru(2)–Ru(2A)	73.58(2)
C(2)–Ru(1)–C(7)	106.9(2)	C(6)–O(6)–Ru(2)	110.8(2)
C(8)–Ru(1)–C(7)	38.95(13)	C(6)–N(1)–C(12)	122.3(3)
C(3)–Ru(1)–Ru(2)	134.90(12)	C(6)–N(1)–C(9)	125.1(3)
C(1)–Ru(1)–Ru(2)	95.51(12)	C(12)–N(1)–C(9)	112.6(3)
C(2)–Ru(1)–Ru(2)	124.53(12)	O(6)–C(6)–N(1)	118.9(3)
C(8)–Ru(1)–Ru(2)	44.73(10)	O(6)–C(6)–C(7)	119.3(3)
C(7)–Ru(1)–Ru(2)	65.39(10)	N(1)–C(6)–C(7)	121.8(3)
C(5)–Ru(2)–C(4)	89.4(2)	C(8)–C(7)–C(6)	116.9(3)
C(5)–Ru(2)–C(8)	96.3(2)	C(7)–C(8)–C(13)	122.8(3)
C(4)–Ru(2)–C(8)	95.1(2)	C(7)–C(8)–Ru(2)	106.9(2)
C(5)–Ru(2)–O(6)	90.7(2)	C(13)–C(8)–Ru(2)	123.8(3)
C(4)–Ru(2)–O(6)	177.69(14)	Ru(1)–H(1)–Ru(2)	105(2)
C(8)–Ru(2)–O(6)	82.58(13)	Ru(1)–H(1)–Ru(2A)	153(2)
C(5)–Ru(2)–Ru(1)	142.78(14)	Ru(2)–H(1)–Ru(2A)	101(2)

Complex **3a** features a quite peculiar planar T-type coordination of hydride ligands (atom H(1) was located directly in the difference Fourier synthesis): the Ru(1)–H(1)–Ru(2), Ru(2)–H(1)–Ru(2A) and Ru(1)–H(1)–Ru(2A) bond angles are equal to 105(2), 101(2), and 153(2)°; the H(1) atom is displaced from the plane of the neighbouring metal atoms by 0.12 Å. In contrast to the pyramidal coordination of the μ_3-hydride ligand which normally occupies the capping position over the triangular face in metal hydride clusters, the planar T-type coordination of the hydride ligand similar to that found in **3a** is very rarely observed. The close analogue which probably presents most interest for structural comparisons, ruthenium hydride complex $Ru_6(\mu\text{-}H)_4(\mu_3\text{-}H)_2(\mu_3,\eta^2\text{-}2\text{-amino-}6\text{-methylpyridine})_2(P(4\text{-tolyl})_3)_2(CO)_{12}$ [10], involves two electron-deficient 46e trinuclear moieties linked by two μ_3-hydride atoms. One may therefore assume that the μ_3-hydride ligands act as a stabilizing factor for electron-deficient transition metal clusters.

The spectroscopic data for complexes **2** (Table 1) are in a good agreement with the results of the X-ray structural study. In the IR spectra of complexes **2** six bands of the carbonyl groups stretching vibrations are observed, their frequencies and relative intensities being practically the same for all complexes.

In the ^1H NMR spectra the =CH–C=O group proton resonance is manifested as a doublet because of the coupling on the bridging hydride. The same coupling of the olefin proton signal was observed in the spectra of analogous complexes obtained earlier from the unsaturated ketones [2]. In the case of complexes **2**, these doublets are shifted towards higher field which is probably due to the presence of electron-donor amino group in the ligand. The chemical shifts and coupling constants of bridging hydrides are quite similar for all complexes **2**. NMR spectra of **2** indicate the hindered rotation of amino group. Indeed, the NMR spectra exhibit different signals for the complexes with identical substituents at the nitrogen atom (NMR spectra of **2b** and **2c**); the complexes with different substituents at the nitrogen atom form the mixture of isomers differing in the orientation of these substituents with respect to the rest of the molecule. Thus, the hindered rotation of the amino group brings about two sets of signals in the NMR spectrum of **2d**. The ratio of the isomers in the mixture, as may be deduced from the relative intensities of the corresponding signals, is equal to 5:1.

Complexes **2**, on heating in hydrocarbon solvents, are converted into the corresponding complexes **3**, which are insoluble in non-polar solvents and precipitate as dark red crystals. One may assume that this process, in fact representing the coupling of binuclear moieties, becomes possible because of the redistribution of electron density in the metallacycle caused by the introduction of the amino substituent. Complexes **3**, as has been mentioned, are electron deficient. When treated with polar solvents, e.g. methylene chloride, they undergo rapid transformations into complexes **2** accompanied by simultaneous partial decomposition.

4. Conclusions

The present work has shown that introduction of the electron-donor amino substituent into the oxadiene groups does not produce major changes in the course of their reactions with dodecacarbonyltriruthenium as compared with their reactions with alkyl- and aryl-substituted oxadienes. In all cases, the products of such reactions involve five-membered oxaruthenacycles η^3 coordinated by the second metal atom as the main structural motif. The amide nitrogen atom never forms the direct coordination bond with the Ru atom. Nevertheless, the presence of the nitrogen-containing substituents gives rise to a substantial redistribution of electron density in the oxaruthenacycle and facilitates the process of coupling of binuclear complexes which leads to tetranuclear species **3**. Tetranuclear complexes of such a type have never been found among the products of the previously studied analogous reactions involving unsaturated ketones without the nitrogenous substituents.

5. Supplementary material

Tables of atomic coordinates, complete bond lengths and angles, anisotropic thermal parameters and observed and calculated structure factors can be obtained from the authors upon request.

Acknowledgements

The authors gratefully acknowledge the financial support of the Russian Foundation for Basic Research (Grant No. 97-03-33783).

References

[1] L.V. Rybin, M.I. Rybinskaya, Russ. Chem. Rev. 62 (1993) 637.
[2] M.I. Rybinskaya, L.V. Rybin, S.V. Osintseva, F.M. Dolgushin, A.I. Yanovsky, Yu.T. Struchkov, Russ. Chem. Bull. 44 (1995) 154.
[3] L.V. Rybin, S.V. Osintseva, P.V. Petrovskii, M.I. Rybinskaya, F.M. Dolgushin, A.I. Yanovsky, Yu.T. Struchkov, J. Organomet. Chem. 479 (1994) C25.
[4] L.V. Rybin, S.V. Osintseva, M.I. Rybinskaya, F.M. Dolgushin, A.I. Yanovsky, Yu.T. Struchkov, J. Organomet. Chem. 485 (1995) 253.
[5] A. Mantovani, S. Cenini, Inorg. Synth. 16 (1976) 47.
[6] H.D. Flack, Acta Crystallogr., Sect. A 39 (1983) 876.
[7] G.M. Sheldrick, SHELXTL Version 5, Software Reference Manual, Siemens Industrial Automation, Madison, WI, 1994.
[8] L.V. Rybin, S.V. Osintseva, A.S. Batsanov, Yu.T. Struchkov, P.V. Petrovskii, M.I. Rybinskaya, Russ. Chem. Bull. 42 (1993) 1228.
[9] F.H. Allen, O. Kennard, D.G. Watson, L. Brammer, A.G. Orpen, R. Taylor, J. Chem. Soc., Perkin Trans. II (1987) S1.
[10] J.A. Cabeza, J.M. Fernandez-Colinas, S. Garcia-Granda, A. Llamazares, F. Lopez-Ortiz, V. Riera, J.F. Van der Maelen, Organometallics 13 (1994) 426.